DOI: 10.1002/ejic.200600087

Structure and Function of Xanthine Oxidoreductase

Russ Hille*[a]

Keywords: Bioinorganic chemistry / Enzymes / Molybdenum / Xanthine / Oxidoreductase

An overview of the current state of our understanding of the reaction mechanism of the molybdenum-containing enzyme xanthine oxidoreductase is presented, with an emphasis on work done in the past five years. Recent studies of the biosynthesis of the pterin cofactor bound to the metal in the active site are also reviewed, as is crystallographic work that has clarified the coordination geometry of the molybdenum center. This structural work provides the context in which to understand recent mechanistic studies of the enzyme, in particular those aimed at elucidating the role of specific amino acid residues in the active site of the enzyme.

Introduction

Xanthine oxidoreductase (until recently also referred to as xanthine oxidase) was first isolated from cow's milk by Dixon and Thurlow some 80 years ago,[1] and was shown to be identical to the so-called Schardinger enzyme responsible for catalyzing the oxidation of aldehydes (reducing redox-active dyes in the process) that had been described even earlier. In 1966, using an elegant ^{95}Mo substitution protocol (and with protein from a very large eukaryote), R. C. Bray showed that the enzyme from cow's milk possessed molybdenum in its active site, and that the metal was reduced to the paramagnetic Mo^{V} state in the course of reduction of substrate.[2] This work provided the first demonstration of a specific biological role for molybdenum. In the intervening years, xanthine oxidoreductase has been the subject of a great many mechanistic, structural and biophysical studies, and has come to represent the paradigm for the molybdenum-containing hydroxylases. Unlike other biological systems that hydroxylate carbon centers (including those that possess flavin, heme, non-heme iron or copper in their active sites), members of this large and phylogenetically diverse family of enzymes utilize water rather than O_2 as the source of the oxygen atom incorporated into product, and generate rather than consume reducing equivalents. These enzymes thus utilize a fundamentally different reaction stoichiometry than the monooxygenases. It is the catalysis of familiar chemistry in an unfamiliar way that has been the principal reason for the continued interest in the reaction mechanism of xanthine oxidoreductase and related enzymes.

The molybdenum hydroxylases constitute by far the largest of the three categories of molybdenum-containing enzymes, with more than 30 discrete members known from sources ranging from hyperthermophilic archaea to higher vertebrates.[3] Most of these enzymes catalyze the hydroxylation of (relatively activated) carbon centers of aromatic heterocycles, but some (like aldehyde oxidase and CO dehydrogenase) catalyze other types of reactions. The human genome encodes four molybdenum hydroxylases: xanthine oxidoreductase proper (expressed under normal circum-

[a] Department of Molecular and Cellular Biochemistry, The Ohio State University,
333 Hamilton Hall, 1645 Neil Avenue, Columbus, OH 43210-1218, USA
E-mail: Hille.1@osu.edu

Russ Hille received a B.S. in Chemistry from Texas Tech University in 1974 and a Ph.D. in Biochemistry from Rice University in 1979. He did post-doctoral work at the University of Michigan in the laboratory of Vincent Massey, in affiliation with the Department of Biological Chemistry and the Michigan Society of Fellows. Afterwards, he took a faculty position in the Department of Molecular and Cellular Biochemistry at The Ohio State University, where he is now Professor. His principal research interests concern the mechanism of action of molybdenum- and flavin-containing enzymes, and biological electron transfer.

MICROREVIEWS: This feature introduces the readers to the authors' research through a concise overview of the selected topic. Reference to important work from others in the field is included.

stances as a NAD^+-reducing dehydrogenase form), and three different aldehyde oxidases [which, like the oxidase form of xanthine oxidoreductase generated under a variety of (patho)physiological conditions, reduce O_2 to either $O_2^{\cdot-}$ or H_2O_2].[4] The aldehyde oxidases appear to represent tissue-specific isozymes that are under different regulation of gene expression. This is certainly the case in higher plants, where one aldehyde oxidase isozyme oxidizes indoleacetaldehyde to the hormone indoleacetic acid, and a second the oxidation of abscissaldehyde to abscissic acid, a second plant hormone.[5] The physiological circumstances under which these two hormones are synthesized are quite distinct and genetic expression of the enzymes involved in the two biosynthetic pathways is under completely separate regulatory control. Thus, while the isolated enzymes may well exhibit considerable overlapping substrate specificity (most members of this family of enzymes exhibit rather broad substrate specificity),[6] under physiological conditions each has a specific physiological reaction for which it is responsible.

What follows is a review of our present understanding of the structure and function of xanthine oxidoreductase. Recent crystallographic studies of the enzyme have refined our understanding of the structure of the active site, particularly with regard to the coordination geometry of the molybdenum center, and this provides the structural context in which the reaction mechanism can be understood – both in the sense of the nature of the chemistry catalyzed and the roles of specific active site amino acid residues in accelerating reaction rate. Before considering these, however, we first review the current status of our understanding of the biosynthesis of the novel pterin cofactor found coordinated to the metal in the enzyme active site. Related subjects, particularly dealing with inorganic systems related to the enzymes of interest here, have been dealt with in recent reviews by other authors.[7–11]

The Pterin Cofactor

With the exception of the extraordinary $MoFe_7$ active site of nitrogenase, molybdenum-containing enzymes all possess an organic pterin cofactor that is coordinated to the metal through an enedithiolate side chain of a third pyran ring, as shown in Figure 1.[12,13] The cofactor is in fact frequently referred to in the literature as molybdopterin, although this is somewhat confusing since: (i) the term refers to the organic component only, not to the metal complexed center; and (ii) the identical cofactor is found in tungsten-containing enzymes – the first crystal structure of an enzyme possessing this cofactor was in fact the tungsten-containing aldehyde oxidoreductase from *Pyrococcus furiosus*.[14] We will use the term pyranopterin here to avoid any possible confusion, but will occasionally use the trivial abbreviation "MPT" (for "*molybdopterin*" or "*metal-binding pterin*"[15]) when convenient. In eukaryotes the cofactor has only the phosphorylated side chain shown, but in many bacterial systems it is elaborated as the dinucleotide of guanosine, cytosine, adenosine or even inosine. As shown in Figure 2, the biosynthetic pathway for the pyranopterin cofactor can be divided into steps leading from GTP to an intermediate initially termed Precursor Z,[16,17] but more recently renamed cyclic pyranopterin monophosphate, cPMP,[18] and then on to the mature cofactor with molybdenum incorporated and (where appropriate in prokaryotes) elaborated to the dinucleotide form. The gene products required for most of the discrete steps are known; many have been crystallographically characterized and their functions are increasingly well understood, as discussed below.

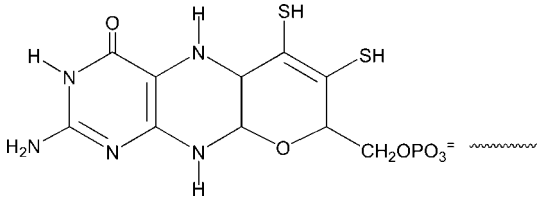

Figure 1. The structure of the pyranopterin cofactor found in molybdenum-containing enzymes. The cofactor consists of a pterin system fused to a pyran ring with a phosphorylated side-chain; molybdenum is coordinated by the dithiolene moiety of the pyran ring. As indicated in the text, the cofactor shown is that seen in eukaryotes. In prokaryotes, it is most often extended as a dinucleotide.

The intermediate cPMP is synthesized from GTP in a reaction that expands the imidazole subnucleus of the guanine moiety to a six-membered pyrazine ring using a carbon from the ribose ring of the nucleotide; the remainder of the ribose ring and α-phosphate group become incorporated into the phosphorylated four-carbon side chain destined to become the pyran ring of the mature cofactor.[19,20] The system responsible for catalyzing this reaction (in *E. coli* consisting of the MoaA and MoaC gene products) is distinct from those involved in biopterin, folate and flavin biosynthesis, and the crystal structures of MoaA[21] and MoaC[22] are each known (Table 1). MoaA is a homodimer, with a [4Fe-4S] cluster in the N-terminal domain that has only three external cysteine ligands to the irons. The missing fourth cysteine position constitutes the binding site for S-adenosylmethionine, with its α-amino and carboxyl groups coordinated to the unique iron site of the cluster in a bidentate fashion. As with other [4Fe-4S]/SAM-containing systems, it is likely that the overall reaction involves reductive cleavage of SAM by the iron-sulfur cluster to initiate a radical-based mechanism for formation of the pterin ring, and specific mechanisms have been proposed.[20,23] A second [4Fe-4S] cluster of unknown function is present in the C-terminal portion of MoaA, and like the N-terminal cluster it lacks one of the external cysteine ligands; the C-terminal [4Fe-4S] cluster lies opposite the active site from the N-terminal [4Fe-4S] cluster and may be involved in binding of GTP, or alternatively in quenching the radical-initiated reaction. The role of MoaC is at present unknown, although it is believed to form a complex with MoaA and may play a role in modulating its activity.[22]

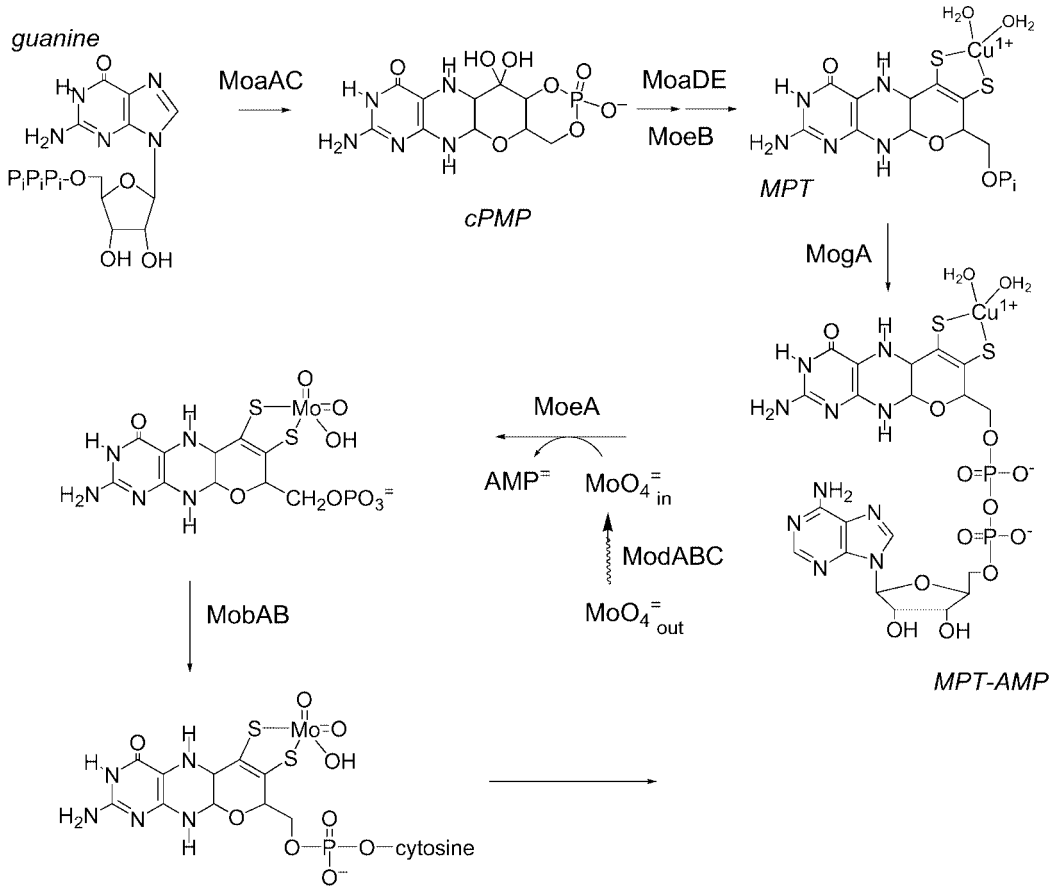

MoaA	cPMP synthesis (2x[4Fe-4S]	ModA	periplasmic $MoO_4^=$ binding protein
MoaB	carrier/insertion protein	ModB	transmembrane channel protein
MoaC	cPMP synthesis	ModC	ATPase
MoaD	MPT synthase α	ModD	chaperone protein
MoaE	MPT synthase β	ModE	$MoO_4^=$-sensitive transcription regulator
MoeA	molybdate insertion into cofactor	MogA	MPT-AMP synthase
MoeB	sulfur charging of MPT synthase	Aba3	sulfido group formation
MobA	pterin dinucleotide synthase α		
MobB	pterin dinucleotide synthase β		

Figure 2. The biosynthetic pathway for the pyranopterin cofactor. Starting from GTP, the key intermediates are: cyclic pyranopterin monophosphate (cPMP), the pyranopterin itself (MPT), and its adenylylated form generated in the course of molybdenum insertion (MPT-AMP).

The structure of cPMP, the product of the MoaAC reaction, was originally thought to be a dihydropterin with a keto (or enol) group at C1′ of the side chain.[19,20] More recently, however, a detailed NMR and mass spectrometric analysis has shown that the pterin ring is fully reduced in cPMP, that C1′ has a geminal diol and that the pyran ring has closed, as shown in Figure 2.[24]

Once formed by MoaAC, cPMP is next doubly sulfurated, a reaction catalyzed by MPT synthase. In *E. coli*, MPT synthase is an $\alpha_2\beta_2$ tetramer consisting of two subunits each of the MoaD (small subunit) and MoaE (large subunit) gene products. Each αβ dimer appears to be functionally independent, with the C-terminal tail of the smaller MoaD subunit inserted into an active site on its partner

Table 1. Orthologues among proteins involved in pyranopterin biosynthesis from various organisms.

E. coli	*A. thaliana*	*H. sapiens*	*Function*
MPT synthesis			
MoaA	Cnx2	MOCS1A	Synthesis of cPMP (2x[4Fe-4S]; SAM)
MoaB			Carrier/insertion protein
MoaC	Cnx3	MOCS1B	Synthesis of cPMP
MoaD	Cnx6	MOCS2B	MPT synthase a (large subunit)
MoaE	Cnx7	MOCS2A	MPT synthase ß (small subunit)
Dinucleotide synthesis			
MobA	–	–	MPT dinucleotide synthase a
MobB	–	–	MPT dinucleotide synthase ß
Molybdate transport			
ModA			Periplasmic molybdate-binding protein
ModB			Transmembrane channel protein
ModC			ATPase
ModD			Chaperone protein
ModE			Molybdate-sensitive transcription regulator
Molybdate insertion, sulfuration			
MoeA	Cnx1(E)		Molybdate insertion into cofactor
MoeB	Cnx5	MOCS3	Sulfur charging of MPT synthase
MogA	Cnx1(G)		MPT-AMP synthase
?	ABA3		Mo=S insertion (into hydroxylases)

MoaE subunit within the tetramer.[25] Interestingly, MoaD has strong structural similarity to ubiquitin, including a C-terminal gly–gly pair, suggesting similar modes of action. Indeed, the overall reaction of MPT synthase involves the formation of an acyl-adenylate at the C-terminus of MoaD (using ATP as the source, by analogy to the mechanism of ubiquitin), with the subsequent formation of a thiocarboxylate. The sulfur atom used to form this thiocarboxylate is delivered by the MoeB gene product, which functions as a biotin-dependent MPT synthase sulfurase and is itself homologous to the E1 family of enzymes involved in adenylylation of ubiquitin.[26] The crystal structure of a $(MoeB)_2$-$(MoaD)_2$ heterotetramer has been reported in several forms, including one in which the C-terminus of MoaD has become adenylylated.[27] For the bacterial system, no evidence has been found for the occurrence of a transiently sulfurated form of *E. coli* MoeB in the course of thiocarboxylate formation, but eukaryotic homologues of MoeB (including the human MOCS3) possess a C-terminal extension with distant homology to rhodanese, and recently it has been shown that Cys 412 of MOCS3 is converted to a persulfide upon incubation with thiosulfate (analogous to the reaction of rhodanese).[28] This persulfide presumably represents the proximal donor of sulfur to the adenylylated MoaD C-terminus, at least in eukaryotic systems. Once charged with sulfur, the synthase first makes a mono-sulfurated form of the pterin (at either C1′ or C2′ of the pterin side chain), at which point it must be recharged with a second sulfur by MoeB prior to completing formation of the dithiolene side chain of the mature pyranopterin cofactor.[29,30]

At least some organisms encode proteins that appear to serve a storage or transport function for the now mature pyranopterin cofactor. Fernandez and co-workers have characterized a protein from *Chlamydomonas rheinhardtii*, for example, that binds pyranopterin and prevents its oxidation.[31–33] The protein is a 64 kDa homotetramer which on the basis of its amino acid sequence is likely to possess a typical nucleotide-binding Rossman fold. Similar proteins exist in both bacteria and higher plants,[33] and may well prove to be widely distributed in nature.

Once the dithiolene moiety is incorporated into the pyranopterin cofactor, molybdenum must be inserted. In *E. coli*, molybdenum is taken up as molybdate by a specific ABC-type transporter system encoded by the *modABCD* operon.[34] The first component of this system is ModA,[35] which has the classic two-domain structure of a periplasmic binding protein.[36] Molybdenum is subsequently transfer-

red to ModB, a peripheral membrane protein in the inner membrane, then internalized to the cytoplasm in an ATP-dependent reaction catalyzed by the membrane-integral ModC gene product.[34] The fourth component of this transport system, the ModD gene product, has an as-yet unidentified function. Recent crystallographic work[37–39] has demonstrated that the process by which molybdate, once in the cell cytoplasm, becomes bound to the pyranopterin cofactor is considerably more complicated than might have been suspected. In particular, solving crystal structures of two forms of the N-terminal Cnx1G domain of the Cnx1 gene product from *A. thaliana* (equivalent to MogA from *E. coli*) in complex with the mature cofactor,[39] it has been shown that the cofactor is first adenylylated to MPT-AMP by Cnx1G, and at this point is coordinated to a copper ion. The cuprated MPT-AMP is then thought to be transferred to the C-terminal Cnx1E domain of Cnx1 (equivalent to MoeA of *E. coli*), which hydrolyzes the dinucleotide in the course of replacing the copper with molybdate. The manner in which this reaction occurs is not yet understood, although the process is known to require magnesium.[39] It is interesting that Cnx1 exhibits significant homology to the mammalian protein gephyrin,[38] a cellular structural element involved in, among other things, neuroreceptor aggregation in certain cell signaling processes.

With molybdate incorporated, the cofactor is in the form seen utilized in two different types of eukaryotic molybdenum enzyme, sulfite oxidase and the assimilatory nitrate reductase, and may now be directly incorporated into the apoproteins. The structure of the center is as indicated in Figure 2, with the molybdenum having a (presumably square-pyramidal) $LMo^{VI}O_2(OH)$, with L representing the bidentate pyranopterin cofactor coordinated to the metal by its enedithiolate side chain. Insertion into apoprotein, which involves replacement of the Mo–OH ligand by a cysteine residue in the active site of the protein, likely involves additional gene products. For example, for some prokaryotic molybdenum enzymes (notably the dissimilatory nitrate reductases and the xanthine dehydrogenase from bacteria such as *R. capsulatus*), cofactor incorporation appears to involve an enzyme-specific "chaperone" protein. The *nar* operon of *E. coli* encodes a NarJ protein that is not a component of the mature protein, but whose deletion prevents proper maturation of the molybdenum center.[40] The XdhC gene product of *R. capsulatus* appears to play a similar role in the maturation of the xanthine dehydrogenase of that organism.[41]

As mentioned above, most prokaryotic enzymes utilize a dinucleotide form of the cofactor, most frequently of guanosine but occasionally of adenosine, cytosine or inosine, which must be generated prior to insertion into the apoprotein. In *E. coli*, MGD ("*M*PT *g*uanosine *d*inucleotide") is synthesized by MGD synthase, which consists of the MobA and MobB gene products.[42] The active site is found in MobA, whose crystal structure has been determined.[43] MobB appears not to be essential for the in vitro synthesis of MGD, although it seems to increase the efficiency of the process in vivo.[44] The dinucleotide form of the cofactor is now ready to be incorporated into appropriate prokaryotic apoprotein. For those enzymes that require two equivalents of the pyranopterin, however, it is not known at present whether incorporation of the second equivalent occurs before or after insertion of the first (with molybdenum attached) into the apoprotein. There is suggestive evidence that the MoeA gene product may play a specific, if as yet unidentified, role in the maturation of *bis*MPT-containing active sites (as discussed by Schwarz[18]).

Once incorporated into the polypeptide, the molybdenum center is in its functional form for those molybdenum enzymes that catalyze oxygen atom transfer reactions (e.g., sulfite oxidase, the nitrate reductases and DMSO reductase). For the molybdenum hydroxylases from both prokaryotic and eukaryotic sources, however, there is a final aspect of maturation: the replacement of one of the two Mo=O groups of the cofactor by a sulfido (Mo=S) group. This sulfuration is strictly required for activity of these enzymes – the so-called desulfo form of enzymes such as xanthine oxidoreductase have been well-characterized and are devoid of catalytic activity.[45,46] In *A. thaliana*, the sulfuration reaction is catalyzed by the ABA3 gene product,[47,48] a pyridoxal phosphate-utilizing enzyme that uses cysteine as the ultimate source of the sulfur atom incorporated into the molybdenum coordination sphere. ABA3 is a homodimer whose subunits fold into distinct N- and C-terminal domains. Pyridoxal phosphate binds to the N-terminal domain, which exhibits considerable homology to the NifS family of gene products, cysteine desulfurases that are involved in the maturation of, for example, iron-sulfur clusters.[49] The ABA3 reaction proceeds with the transient formation of a cysteine persulfide at Cys 430 of ABA3, which then transfers its terminal sulfur to the molybdenum center,[50] and there is evidence to suggest that the sulfur is transferred transiently to the C-terminal domain of ABA3. This appears not to be an essential step, however: deletion of the C-terminal domain of ABA3 compromises the effectiveness of sulfur incorporation, but does not eliminate it altogether. Interestingly, ABA3 is also able to utilize selenocysteine as substrate,[51] raising the possibility of preparing selenido forms of the hydroxylases which may have interesting catalytic properties.

The Structure of the Active Site of Xanthine Oxidoreductase

The molybdenum hydroxylases are fairly complicated systems as enzymes go, since in addition to the molybdenum center, all members of this family possess additional redox-active centers. The typical constitution is a pair of [2Fe-2S] clusters of the spinach ferredoxin variety and, usually, FAD as well (see Figure 3 for the structure of the bovine xanthine oxidoreductase). In most enzymes, all these prosthetic groups are to be found in discrete domains within a single subunit of an α_2 dimer, although in the *R. capsulatus* xanthine dehydrogenase the iron-sulfur centers and FAD are found in one subunit and the molybdenum

center in a second within an $\alpha_2\beta_2$ tetramer.[51] In the CO dehydrogenase from *O. carboxydovorans* [52] and the quinoline-2-oxidoreductase from *Pseudomonas putida*,[53] the two iron–sulfur centers, the FAD and the molybdenum center are found in separate subunits within an $\alpha_2\beta_2\gamma_2$ hexamer. It is evident from an inspection of the genes encoding these proteins from a variety of organisms that they were built up in gene duplication/fusion events over the course of evolution: not only do the protein domains fold into autonomous structural elements, but they are encoded by contiguous stretches of the gene.

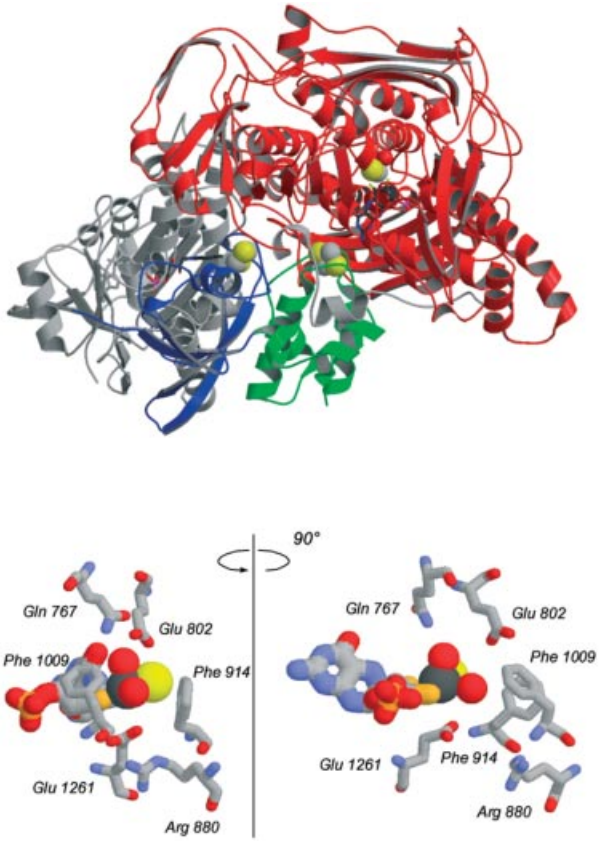

Figure 3. The structure of bovine xanthine oxidoreductase. Top, the overall domain fold of the enzyme, with (from the N-terminus): the two [2Fe–2S] domains in blue and green; the FAD domain in gray (the FAD is shown edge-on, immediately to the left of the first iron-sulfur cluster); and the molybdenum-binding portion of the protein in red. The illustration was prepared with the application MOLSCRIPT, using the structure reported by Enroth et al.[99] Bottom, two representations of the active site with specific amino acid residues discussed in the text indicated.

The first molybdenum hydroxylase to be crystallographically characterized was the aldehyde oxidoreductase from *Desulfovibrio gigas*.[54,55] Several important structural features of the enzyme were established in this work, including: the overall domain architecture of the protein (with the two [2Fe–2S] clusters of the enzyme in separate N-terminal domains and the molybdenum center at the interface of two much larger C-terminal domains); the orientation of the molybdenum center with respect to the remaining redox-active centers of the enzyme (including the hydrogen-bonding interaction between the distal amino group of the pyranopterin cofactor to one of the cysteine ligands of the nearer [2Fe–2S] cluster); the identity of specific amino acid residues in the active site likely to be involved in catalysis (including, most importantly, a highly conserved glutamate residue that was suggested to function as an active-site base[55] – see Figure 3, *bottom* for the active site of the bovine xanthine oxidoreductase); the overall square-pyramidal coordination geometry of the molybdenum coordination sphere, with an $LMoO_2(OH_{(2)})$ coordination geometry and a hydroxy/water ligand that points toward the substrate binding site; and the long channel that provides solvent access to the deeply buried active site. Unfortunately, the *D. gigas* aldehyde oxidoreductase is an example of the molybdenum hydroxylases that does not possess FAD, and the structure provided no information regarding the flavin site found in most other molybdenum hydroxylases. More importantly, the enzyme used in this initial crystallographic study was predominantly in the inactive desulfo form and lacked the catalytically essential Mo=S group. It was not possible to say which of the two Mo=O groups present in the molybdenum coordination sphere of the desulfo form (one in the apical position and the other in an equatorial position) was the one that was replaced by a sulfido group in the functional enzyme. A subsequent study of (partially) activated enzyme, obtained by treating crystals with a resulfurating agent, suggested on the basis of electron density analysis that is was the apical Mo=O that was replaced by sulfur to become Mo=S.[55] This assignment is surprising from the standpoint of the known coordination chemistry of model molybdenum complexes – inevitably, a single Mo=O group is located in the apical position within a square-pyramidal coordination sphere, opposite the vacant ligand position, owing to its strong *trans* effect. This being the case, one would have expected the equatorial position to be substituted by sulfur, not the apical one. Indeed, the magnetic circular dichroism electron of a catalytically relevant Mo^V form of xanthine oxidoreductase, that giving rise to the "very rapid" EPR signal (see below), is virtually identical to that exhibited by simple model complexes known to have an apical Mo=O, indicating that the enzyme has an electronic (and presumably also physical) structure fundamentally the same as the crystallographically defined model complexes.[56]

More recently, three other enzyme crystal structures have become available that strongly indicate it is indeed the equatorial position that becomes sulfurated upon activation in the molybdenum hydroxylases. The first of these is that of the molybdenum-containing CO dehydrogenase from the aerobic *Oligotropha carboxydovorans* (as opposed to the Ni-containing enzyme from anaerobes such as *Methanosarcina thermophila* or *Rhodospirillum rubrum*[57,58]). This enzyme is an interesting variation on the theme of the molybdenum hydroxylases, with a binuclear Mo/Cu active site.[59,60] In the crystal structure,[59] the copper ion occupies a position in the equatorial plane of the molybdenum coordination sphere, connected to the molybdenum itself by a bridging

acid-labile sulfur that is analogous to the catalytically essential sulfur of other members of this enzyme family. Although unique among the molybdenum hydroxylases characterized to date in possessing a binuclear center, the active-site structure of CO dehydrogenase is clearly related to those of other members of this class of enzyme, and the position of the copper site suggests an equatorial Mo=S in the other enzymes. The second structure is that of the *P. putida* quinoline-2-oxidoreductase, where a careful analysis of the structure of the molybdenum center in the oxidized enzyme indicated an apical Mo=O at 1.69 Å and an equatorial Mo=S at 2.13 Å.[53] The third structure is that of a high-specific activity preparation of the (reduced) bovine oxidoreductase in complex with a potent mechanism-based inhibitor termed FYX-051.[61] This inhibitor is actually a substrate for the enzyme, but once hydroxylated becomes very tightly bound to the reduced enzyme in a classic mechanism-based mode of enzyme inhibition. In the crystal structure of this complex, it is abundantly clear that it is the equatorial position, adjacent to the bound inhibitor (which is coordinated to the molybdenum center through the newly introduced hydroxy group of the product), that has the added electron density of sulfur and not the apical position. On the basis of the present evidence, it thus seems clear that the apical position of the molybdenum centers in the molybdenum hydroxylases is an Mo=O, with an equatorial Mo=S in the oxidized from of the enzyme (or Mo–SH in the reduced form, see below).

The Reaction Mechanism of Xanthine Oxidoreductase

The structure of the molybdenum center of xanthine oxidoreductase (Figure 3, *bottom*) provides the structural context in which to understand the reaction mechanism of the enzyme. It had been known for many years that the active site began in a $Mo^{VI}OS$ oxidation state and at the completion of the reaction was reduced by two equivalents and protonated at the Mo=S group to give a $Mo^{IV}O(SH)$.[62,63] Rather more recently it was also shown that a proximal site on the enzyme was the source the oxygen atom incorporated into product;[64] this site was regenerated with oxygen from solvent (i.e., already reduced to the level of water) at the completion of each catalytic cycle.[65] It has subsequently been demonstrated that ^{17}O from water exchanges into the molybdenum center rapidly under turnover conditions, and that the site labeled is strongly and anisotropically coupled to the molybdenum when in the Mo^{V} valence state.[66] From a comparison with model compounds of known structure,[67] the labeled site corresponds to the equatorial Mo–OH rather than the equatorial Mo=O site. A similar conclusion has been drawn from the inability to observe a second, more weakly ^{17}O coupling in the "very rapid" EPR signal underneath the stronger coupling of the Mo–O-product oxygen under conditions when the molybdenum should have become labeled catalytically.[68] It is noteworthy that although initially assigned as a bound water molecule on the basis of the crystallographically determined Mo–O distance in the *D. gigas* aldehyde oxidoreductase structure, a more precise determination of this distance using X-ray absorption spectroscopy with the bovine xanthine oxidoreductase indicates that at 2.1 Å it is in fact a hydroxide ligand.[69] This is actually a fairly important mechanistic point, because a Mo–OH group deprotonated to $Mo–O^-$ is expected to be a considerably better nucleophile in initiating catalysis than would be a $Mo–OH_2$ group deprotonated to Mo–OH (see below). The protonation of the Mo=S group upon reduction of the molybdenum center in going from an $LMo^{VI}OS(OH)$ to an $LMo^{IV}O(SH)(OH)$ center is consistent with the concept of electroneutrality – that the protein environments of metal centers are designed to accommodate a specific net charge, and that changes in charge associated with reduction tend to be compensated by uptake of protons at or near the metal center. The uptake of protons by ligands to molybdenum upon reduction of the metal is in fact a property of even the simplest molybdate complexes.[70,71]

Other clues as to the chemical course of the reaction of xanthine oxidoreductases come from studies of the reaction of enzyme with the (poor) substrate 2-hydroxy-6-methylpurine. Although turnover with this substrate is some 10^3-fold slower than with xanthine, the reaction (at least at high pH) proceeds with sequentially smaller rate constants associated with each of several steps in the catalytic sequence.[72] The result is that two reaction intermediates accumulate to an appreciable degree. The first of these has an absorption maximum (relative to oxidized enzyme) at 470 nm in the visible region, and upon *oxidation* by one equivalent is converted to a second species with an absorption maximum at 540 nm.[72] Formation of this latter species is coincident with the accumulation of the EPR-active Mo^{V} state giving rise to the "very rapid" signal referred to above. This signal, so named on the basis of the kinetics of its formation and decay in the course of the reaction of enzyme with xanthine,[73,74] has long been recognized to be a fully competent catalytic intermediate. The implication of the work with the hydroxymethylpurine substrate is that the 470 nm-absorbing species must be the Mo^{IV} species from which the Mo^{V} species arises, and that the initial step of the reaction involves the two-electron reduction of the molybdenum center. Further, since earlier work had demonstrated that weak coupling to ^{13}C (I = 1/2) is observed in the "very rapid" EPR signal when the sample is prepared using 8–^{13}C-labeled substrate,[75] the purine nucleus must be present in the EPR-active species (and hence also in its mechanistic precursor). The final mechanistically relevant observation is that the Mo–O bond of product has formed at the point of formation of the Mo^{IV} species: acid quenching of the reaction mix at the point of maximum accumulation of this species followed by work-up affords the hydroxylated product of the reaction and not substrate.[72]

Under the conditions used, with 2-hydroxy-6-methylpurine as substrate and at pH 10, the entirety of the catalytic throughput passes through the "very rapid" EPR-active

state, and the integrated EPR intensity at maximum accumulation of the species (approximately 85% of the functional enzyme) agrees well with that expected given the observed rate constants for formation and decay of the species (1.0 and 0.1 s^{-1}, respectively, at 25 °C). With other substrates, and at other reaction conditions, however, the observed accumulation of this EPR-active state is significantly smaller than expected on the basis of the observed rate constants for formation and decay of the "very rapid" species.[76,77] The most likely explanation is that the reaction mechanism is bifurcated at the point of the Mo(VI)*P intermediate that precedes the "very rapid" species; oxidation by one electron yields the EPR-active species, but alternatively product may dissociate prior to oxidation of the Mo^{IV} with the result that the "very rapid" species does not form. On the basis of the amount of "very rapid" signal accumulating under a variety of conditions with a wide range of substrate, it is evident that the fraction of total catalytic flux that passes through the EPR-active "very rapid" species is in fact usually quite small.

While the "very rapid" species may arise in only a relatively small fraction of turnover events, it nevertheless provides an important opportunity to understand the structure of the Mo^{IV} state that precedes it, and this Mo^{IV} species appears to be an obligatory catalytic intermediate. The "very rapid" EPR signal is devoid of proton superhyperfine splitting and has strong, anisotropic coupling to ^{33}S when enzyme is appropriately labeled, consistent with the existence of an Mo^{V}=S unit.[78] Strong but isotropic coupling is also observed when the sample is prepared in ^{17}O-labeled water,[79] interpreted as evidence for a Mo–O product species. Overall, EPR work had thus early on provided strong evidence that the "very rapid" species possessed a MoOS(O-product) structure.

As indicated above, when the "very rapid" species is generated using substrate that has been labeled at C_8, weak superhyperfine coupling is seen in the EPR signal due to the I = 1/2 spin of the ^{13}C nucleus. This permits a distance from the carbon to the molybdenum to be obtained from the anisotropy of the coupling as ascertained by ENDOR spectroscopy. An initial study arrived at a short Mo–C distance – ca. 2.4 Å or shorter – which was interpreted as evidence in favor of a direct metal–carbon bond.[68] Subsequent work, however, has demonstrated convincingly that the distance is no shorter than 2.8 Å, indicating that the carbon is in the second coordination shell of the molybdenum rather than the first.[80] Further, although no proton superhyperfine is evident in the "very rapid" EPR signal, weak coupling to two sets of protons is seen using electron spin echo spectroscopy and as in the case with ENDOR distances can be estimated from the molybdenum: the results of the analysis indicate a single proton at ca. 2.4 Å and a set of two or more at ca. 6.1 Å (from the methyl group of the 2-hydroxy-6-methylpurine substrate that was used in the study).[81] With the Mo–C distance obtained from the ENDOR experiments above, it is possible to triangulate and obtain the orientation of the purine nucleus relative to the molybdenum atom. The data are consistent with binding of the (now hydroxylated) purine nucleus directly to molybdenum in an end-on fashion by the catalytically introduced hydroxy oxygen (Figure 4).

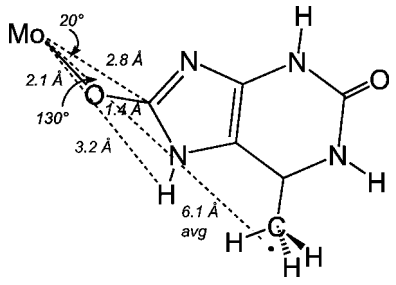

Figure 4. The structure of bound product to the molybdenum in the active site of xanthine oxidoreductase. The structure shown is for the product of the enzyme reaction with the slow substrate 2-hydroxy-6-methylpurine, which was used in the work. The Mo–C distance was obtained by ENDOR spectroscopy with 8-^{13}C-labeled substrate as substrate,[80] and the Mo–H distances by ESEEM spectroscopy,[81] as discussed in the text.

The above work using MCD, EPR and related methods to probe the Mo^{V} state of the molybdenum center has been used to infer the structure of the preceding Mo^{IV} intermediate in the catalytic sequence. Happily, with certain substrates of the enzyme this intermediate can be prepared in a stable form simply by addition of the hydroxylated product to enzyme that has been non-catalytically reduced by a reagent such as sodium dithionite. The best characterized case is that of violapterin, the product of enzyme action on the pteridine substrate lumazine (2,6-dihydroxypteridine). Addition of violapterin to reduced enzyme results in formation of a Mo^{IV}-containing reduced enzyme–product complex (E_{red}·P) that exhibits a relatively strong and broad charge-transfer transition centered at 640 nm.[82–84] This characteristic long-wavelength absorbance has been used in kinetic experiments to demonstrate that the charge-transfer complex is indeed an authentic catalytic intermediate.[83] The inhibitor FYX-051 used in the crystallographic work described above is another substrate that forms such a charge-transfer complex, and it is the E_{red}·P complex formed with this substrate whose structure has recently been reported.[61] In addition to establishing that the sulfido sulfur of the active form of the enzyme is in the equatorial rather than apical position, this work unambiguously shows product coordinated end-on to the molybdenum atom by the catalytically introduced hydroxy oxygen in a manner comparable to that shown in Figure 4. The position in the molybdenum coordination sphere is that occupied by the Mo–OH group of oxidized enzyme, lending further support to the conclusion that the Mo–OH represents the catalytically labile oxygen in the active site. Wedd and co-workers had in fact previously suggested that the catalytically labile oxygen could be a molybdenum-bound hydroxide.[67] The simple end-on binding of product (which formally is in the enolate tautomer at C^7, the site that has become hydroxylated) contrasts with other proposals where product, in the keto tautomer, binds side-on (a so-called η_2 interaction with

the molybdenum) with partial formation of a Mo–C bond.[68] It is evident from the crystal structure that such a binding mode is sterically impossible in the active site.

The evidence thus summarized above indicates that the Mo^{IV} species is formed in the first step of the catalytic sequence: the molybdenum has been reduced from Mo^{VI} to Mo^{IV}, the O–C bond of product formed and the Mo=S of oxidized enzyme protonated to Mo–SH, all simultaneously. An important clue as to the chemical mechanism by which the E_{red}·P intermediate is generated comes from the pH dependence of its formation, as reflected in the kinetic parameter k_{cat}/k_m from steady-state experiments (or equivalently, since the rate-limiting step for turnover is known to be in the reductive half-reaction, k_{red}/K_d from rapid reaction studies following the rate of reduction of enzyme by excess xanthine as a function of substrate concentration). The pH profile for both kinetic parameters track the reaction of free enzyme with free substrate through to the formation of the E_{red}·P complex; it is bell-shaped with a pK_a for the acid limb of 6.6 and for the alkaline limb of 7.4.[85] The latter value agrees very well with the pK_a for the first ionization of substrate, indicating that enzyme acts on the neutral rather than monoanionic form of substrate. This is expected if the reaction is initiated by nucleophilic attack, since a negative charge on substrate would compromise this first step of catalysis. The former pK_a has been assigned to Glu 1261 in the active site of the enzyme, the same highly conserved glutamate first seen in the crystal structure of the *D. gigas* aldehyde oxidoreductase and proposed to be the active-site base.[55] The implication is that the glutamate must be unprotonated prior to the onset of catalysis, as should be the case if its role is to abstract a proton from substrate to initiate the catalytic sequence.

The chemical mechanism for formation of the initial E_{red}·P complex that emerges from all of the above is one in which the reaction is initiated by base-catalyzed abstraction of a proton from the Mo–OH group by Glu 1261, followed by nucleophilic attack of the oxyanion thus generated on the C^8 of substrate. Concomitant hydride transfer to the Mo=S group in the equatorial plane of the molybdenum coordination sphere generates E_{red}·P as shown in Figure 5. Direct hydride transfer to the Mo=S in the course of the reaction is consistent with the observation of Bray and Knowles that the C^8–H proton of substrate is initially transferred to the molybdenum center, and only subsequently exchanges with solvent.[86] Since both pairs of electrons in the Mo=S bond belong to the sulfur in a formal valence count, conversion of Mo=S to Mo–SH with this hydride transfer brings about the formal two-electron reduction of Mo^{VI} to Mo^{IV}. The reaction is completed by electron transfer from the molybdenum to the other redox-active centers of the enzyme and deprotonation of the Mo^{IV}–SH group. Displacement of bound product by hydroxide from solvent may occur prior to transfer of the first electron out of the molybdenum center or after (in which case the "very rapid" species is generated).

A reaction predicated on nucleophilic attack on the heterocycle nucleus had in fact been suggested previously be Lee and Skibo,[87] who showed that for enzyme acting on a homologous series of substituted quinazoline substrates, a linear correlation existed between $\log(k_{cat}/K_m)$ and the pK_a of the quinazoline (at least for substrates having a pK_a > 9). The implication was that, as with xanthine, the substrate was required to be in the neutral rather than monoanionic form for the reaction to proceed. In addition, a variety of computational studies of the reaction mechanism are fully consistent with a mechanism involving concomitant nucleophilic attack and hydride transfer.[88–91] In the earliest of these studies, Voityuk and co-workers[88] showed that the Mo–OH form of a model for the molybdenum center was considerably more stable than a Mo–OH_2 form, an important observation because deprotonating the latter species (to Mo–OH) is unlikely to generate a sufficiently effective base as to function catalytically, as discussed above. Subsequent work by this same group[89] examined the reaction of the model (surprisingly, starting from a Mo–OH_2 species rather than the more stable Mo–OH shown in their previous study) with formaldehyde, a known inhibitor of xanthine oxidoreductase. The work implicated a reaction mechanism involving hydride transfer from the substrate to the Mo^{VI}=S, yielding Mo^{IV}–SH, in the course of the nucleophilic attack on substrate. Working with a similar model for the enzyme molybdenum center, but importantly starting with a Mo–OH rather than Mo–OH_2 species, Ilich et al.[90] established the same two points (i.e., nucleophilic attack on substrate with concomitant hydride transfer to the Mo=S) for the reaction of the model with the bona fide enzyme substrate formamide (which is hydroxylated to carbamate). Most significantly from this study, the transition state was well-defined, permitting the unambiguous demonstration of partial negative charge on the hydrogen being transferred and indicating hydride-like character.[90] Subsequent work with the same system provided a rationale as to why substitution of a second Mo=O group for the Mo=S of functional enzyme resulted in loss of activity: the transition state for the reaction of the MoO_2 model was found to lie considerably earlier along the reaction coordinate than with the MoOS model and at approximately 13 kcal/mol higher in energy (corresponding to a reduction in rate of over nine orders of magnitude as compared with the sulfido form).[91] Interestingly, although calculations with a putative selenated form of the model (MoOSe) did not converge, those with a tellurated form (MoOTe) were successful and suggested that such a form of the enzyme should exhibit even greater reactivity than the naturally occurring MoOS form.[91]

Finally, it has been suggested that the initial E_{red}·P complex forms through a radical mechanism rather than the two-electron chemistry implicit in a mechanism involving nucleophilic attack, with rate-limiting formation of a (presumably extremely unstable) Mo^{V}···xanthine$^{\cdot+}$ diradical species upon direct one-electron transfer from substrate to molybdenum in the Mo^{VI}···xanthine Michaelis complex.[92] Were this the case, however, a linear relationship should exist between the substrate/substrate$^{\cdot+}$ one-electron reduction potential and reaction rate. Examining a homologous series

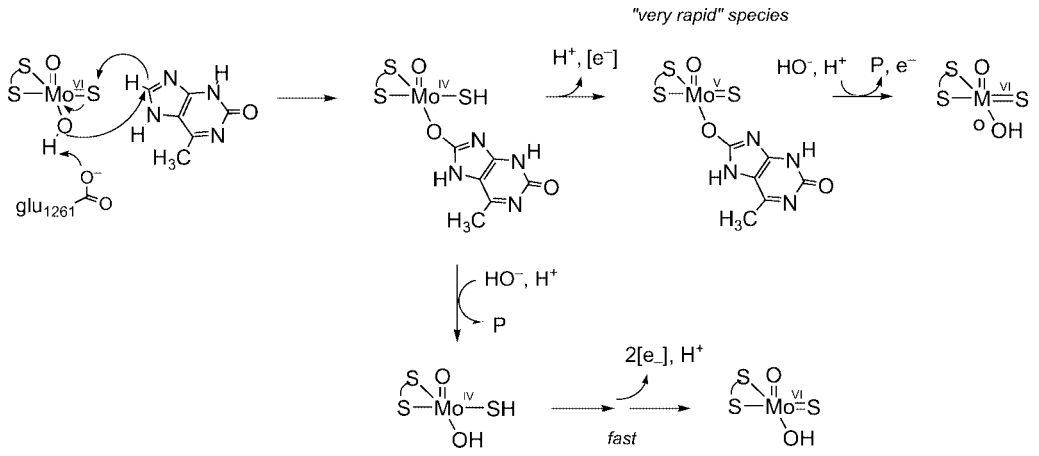

Figure 5. The reaction mechanism of xanthine oxidoreductase. The reaction involves base-assisted nucleophilic attack on the C^8 position of substrate, with concomitant hydride transfer to the Mo=S group of the oxidized enzyme and reduction of the molybdenum itself by two equivalents. From the initial E_{red}·P intermediate, the molybdenum may become oxidized (by electron transfer to the other redox-active centers of the enzyme) and deprotonated to form the species giving rise to the "very rapid" EPR signal as discussed in the text, or alternatively hydroxide may displace product from the molybdenum coordination sphere, followed by subsequent reoxidation of the molybdenum.

of purine substrates for xanthine oxidoreductase, Stockert et al. failed to observe such a relationship[93] arguing strongly against a radical-based mechanism and leaving the two-electron chemistry shown in the proposed reaction predicated on nucleophilic attack as the most likely mechanistic alternative. It is worth noting that for the molybdenum-containing aldehyde oxidases a reaction mechanism involving nucleophilic attack on the aldehyde carbonyl moiety had long been the preferred reaction mechanism for oxidation of aldehydes to carboxylic acids. It thus appears that the two principal subclasses of the molybdenum hydroxylases (those that act on aromatic heterocycles and those that act on aldehyde substrates) utilize fundamentally the same mechanism to accelerate reaction rate. This goes a long way in explaining the extremely broad and overlapping substrate specificities of the mammalian xanthine oxidoreductases and aldehyde oxidases.

The Roles of Specific Amino Acid Residues in Catalysis

On the basis of the above, there is broad experimental support for a reaction mechanism initiated by nucleophilic attack, and in the past five years such a mechanism (Figure 5) has received general acceptance in the field. It is significant that computational studies, involving minimal structures for both the molybdenum center and substrate and not including the protein structure at all, have successfully defined the trajectory of the system across the potential energy surface that defines the reaction. This indicates that the course of the reaction is dictated by the electronic structure of the metal center itself; that is, the reactivity of the enzyme is an intrinsic property of the metal center. Having said this, it is evident that (as in all enzymes) the polypeptide (and specific amino acid residues in the active site of the enzyme in particular) is crucially involved in lowering the energies of the transition states encountered along this trajectory, in some cases enormously so. The structure of the active site of bovine xanthine oxidoreductase is shown in Figure 3, with several specific amino acid residues that are likely to play a role in catalysis indicated. Glu 1261 (in the bovine enzyme sequence) has already been referred to as the candidate active-site base that initiates nucleophilic attack on substrate. This residue is universally conserved in the molybdenum hydroxylases, both in those enzymes hydroxylating aromatic heterocycles and in the aldehyde oxidases. In addition, a second glutamate (802 in the bovine enzyme) is conserved in the heterocycle-hydroxylating enzymes, but not in those that have aldehydes as substrates. Other residues that are conserved in the heterocycle-hydroxylating enzymes, (but not always in those that act on aldehydes) include the two phenylalanine residues between which the aromatic substrate is sandwiched on binding in the active site (914 and 1009 in the bovine enzyme), Gln 767 which is within hydrogen-bonding distance of the apical Mo=O, and Arg 880, which appears to interact with the distal end of substrate opposite the C^8 position that becomes hydroxylated. We consider now the results of recent studies of the roles of these active-site residues in two recombinant systems that have been developed for site-directed mutagenesis studies: the bacterial xanthine dehydrogenase from *Rhodobacter capsulatus* (as expressed in *E. coli*)[94] and the rat xanthine oxidoreductase, as expressed in insect cells using the baculovirus vector.[95]

The residues that have been examined to date are the two glutamates in the active site. Leimkühler et al.[96] have mutated both Glu232 and Glu730 in the xanthine dehydrogenase from *R. capsulatus* to alanine (these residues correspond to Glu 802 and Glu1261, respectively, in the bovine enzyme). The E232A mutant exhibits considerably reduced activity, with the limiting rate of reduction of enzyme by

xanthine in rapid kinetic experiments decreased from 67 s^{-1} for the wild-type enzyme to 5.5 s^{-1} for the mutant. The K_d is correspondingly affected, increasing from 34 μM to 410 μM. It is evident that the free energy associated with the interaction of this residue with substrate, ca. 3 kcal/mol, is used approximately equally to bind substrate on the one hand, and lower the activation barrier for the reaction on the other. The result is that k_{red}/K_d (the effective second-order rate constant of free enzyme with free substrate in the lower [S] regime) is compromised by over two orders of magnitude in the mutant enzyme. The E730A mutant is profoundly compromised in reactivity toward substrate – no reduction of enzyme was detected in an overnight incubation with excess xanthine under anaerobic conditions (with wild-type enzyme, the reaction is complete in less than 200 ms under the conditions). Control experiments established that the mutant enzyme had only about 30% functional active sites (based on molybdenum and sulfur content), but still the absorbance change associated with reduction of the active enzyme should have been easily detected. Further, other mutants (notably E730Q and E730R) had more molybdenum and sulfur incorporated, but were similarly inactive. Conservatively, the E730A mutant has a lower limiting rate of reduction by substrate of at least 10^7 compared to wild-type enzyme, indicating that this residue contributes at least 10 kcal/mol toward transition state stabilization in the reduction of enzyme by substrate. Clearly, this residue is essential for catalysis, consistent with its proposed role as an active base initiating the reaction. Unfortunately, it was not possible to carry out a "chemical rescue" of the E730A mutant by addition of acetate (which conceivably might have bound in the empty pocket otherwise occupied by the glutamate side chain, possibly restoring at least some activity) and an E730G mutant is not stable (S. Leimkühler, unpublished). It thus remains to be established that Glu 730 functions specifically as an active-site base in the course of the reaction.

Resonance Roman Studies of the Molybdenum Center of Xanthine Oxidoreductase

The above site-directed mutagenesis studies illustrate how interactions between substrate and enzyme can be mapped out in the active site, and rapid reaction kinetic studies used to quantitate the extent to which the free energy associated with these interactions is used to either bind substrate (i.e. influence K_d) or accelerate reaction time (i.e. influence k_{red}). It is also possible to probe enzyme-substrate interactions using resonance Raman spectroscopy, which provides detailed information about the vibrational frequencies (and hence bond strengths) of bonds in chromophores. The method is particularly useful when applied to metalloproteins, where by virtue of resonance enhancement it is frequently possible to focus on just those bonds in the active site, ignoring those of the polypeptide in general. In the case of xanthine oxidoreductase, Kitagawa, Nishino and co-workers have examined the as-isolated, oxidized enzyme by resonance Raman spectroscopy and identified specific vibrational modes attributable to ligands to the metal, in particular the Mo=O and Mo=S stretching frequencies at 899 and 474 cm^{-1}, respectively.[97] Interestingly, while substitution of the Mo=S with ^{34}S was facile, the Mo=O group could not be exchanged with solvent $H_2{}^{18}O$ even under rather extreme reaction conditions, indicating that the apical oxo group is stable and does not readily exchange with solvent. Other vibrational modes due to the [2Fe–2S] clusters and FAD of the enzyme were assigned, but no modes attributable to the enedithiolate ligand to molybdenum could be identified.

Advantage can also be taken of the long-wavelength absorption of the E_{red}·P complex seen with violapterin that was discussed earlier to use resonance Raman as an active-site probe. As illustrated in Figure 6 (bottom) the (ordinary) Raman spectrum of violapterin is significantly perturbed on binding to the reduced enzyme (top).[98] Apart from the differences in band intensity, which have largely to do with the fact that only certain modes seen in the E_{red}·P complex are resonance-enhanced (while those of the violapterin in free solution are not), it is evident that almost every mode seen in the spectrum of violapterin is shifted in the enzyme complex to at least a small extent. The principal reason for this is that while both the free and enzyme complexed forms are monoanionic under the experimental conditions, the free violapterin has the negative charge accumulated in the N_3 region of the pyrimidine subnucleus, while in the enzyme complexed formal negative charge accumulates to a much greater extent at the C^7–O, which coordinates to the molybdenum [by analogy to the crystal structure of the E_{red}·(FYX-051) complex]. Two of the most prominent vibrational modes in the free violapterin monoanion, at 704 and 1286 cm^{-1}, are shifted modestly (to 699 and 1294 cm^{-1}, respectively), and the third, at 1379 cm^{-1}, is greatly diminished in intensity. The shifts are on the order expected for increased negative charge accumulation at the C^7–O upon binding the enzyme. A normal mode analysis of the E_{red}·P complex indicates that the bands seen at 699, 852, 1294 and 146 cm^{-1} vibrations have motions that include significant ring deformation.[98] In addition, the set of modes in the 1550–1700 cm^{-1} region can be assigned to a second group of vibrations that have major contributions by C^2=O and C^4=O stretching motions. It is interesting that when the sample is prepared in such a way as to label the bridging oxygen between C^7 of the pterin nucleus and the molybdenum that the two most isotope-sensitive modes are those seen at 1467 and 1563 cm^{-1}, shifting 12 and 15 cm^{-1}, respectively, to lower energy with the heavier isotope.[98] That both these modes lie to considerably lower energy than expected for a typical carbonyl group is consistent with the C^7–O bond having significant single-bond character in the enzyme-bound product.

With the mode assignments for specific experimentally observed vibrational bands that have been made to date,[98] it is possible to begin to map out the regions on the heterocycle that interact with specific amino acid residues in the

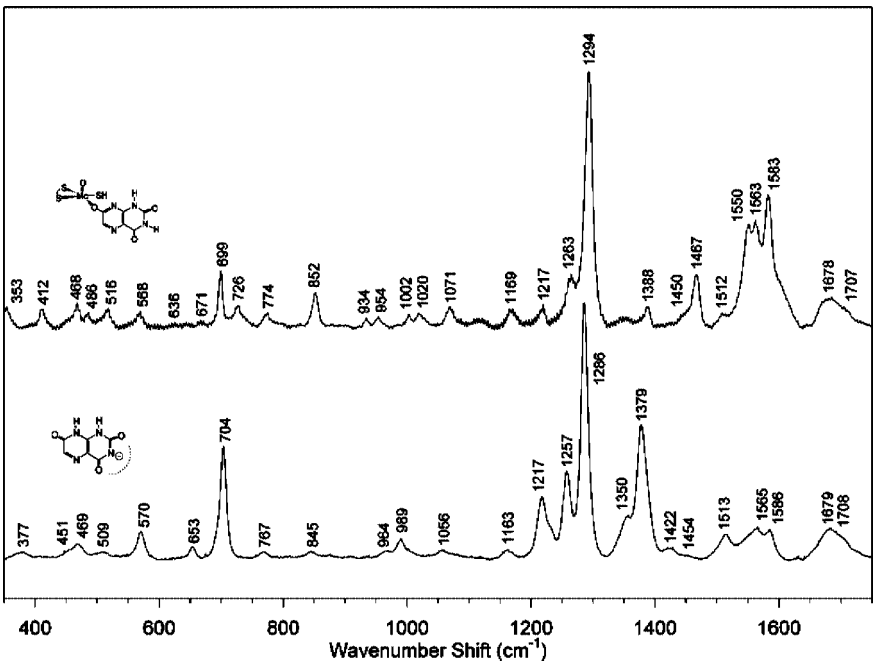

Figure 6. Resonance Raman spectra of the monoanion of violapterin (bottom) and the complex of reduced enzyme with violapterin (top). The spectra were obtained using 647-nm excitation.

active site and, importantly, quantify the amount of free energy associated with each interaction using site-directed mutagenesis. It is to be expected that work along these lines in the immediate future will provide a quantitative map of enzyme-substrate interactions, which can be correlated with changes in reactivity among the set of enzyme mutants.

Prospectus

The crystal structures of an increasing number of members of the molybdenum hydroxylase family of enzymes have become known, and both the common and unique structural elements of these enzymes identified. There is an emerging consensus regarding the fundamental nature of carbon center hydroxylation as catalyzed by enzymes such as xanthine oxidoreductase, and the specific roles of active site amino acid residues in accelerating reaction rate at each of the several steps of this mechanism are increasingly well understood. The continued application of site-directed mutagenesis will very likely further our understanding of the catalytic process in the near future, and computational approaches in conjunction with spectroscopic methods such as resonance Raman can be expected to advance our understanding of the electronic as well as physical structures of intermediates and transition states. Finally, it can be hoped that new enzymes similar to CO dehydrogenase will be identified whose active-site structures and reaction mechanisms represent interesting variations on the theme for these enzymes that reflect the diversity of chemistry available to molybdenum in a biological context.

[1] M. Dixon, S. Thurlow, *Biochem. J.* **1924**, *18*, 976.
[2] R. C. Bray, L. Meriwether, *Nature* **1966**, *212*, 467.
[3] R. Hille, *Chem. Rev.* **1996**, *96*, 2757.
[4] R. Hille, T. Nishino, *FASEB J.* **1995**, *9*, 995.
[5] M. Seo, A. J. Peeters, H. Kiowai, T. Oritani, A. Marion-Poll, *Proc. Natl. Acad. Sci. USA* **2000**, *97*, 12908.
[6] V. Massey, in *Iron-Sulfur Proteins*, vol. 1 (Ed.: A. Ehrenberg), Academic Press, New York, **1973**, pp. 301–360.
[7] J. M. Tunney, J. McMaster, C. D. Garner, in *Comparative Coordination Chemistry II* (Eds.: J. A. McCleverty, T. J. Meyer), vol. 8, p. 459, Elsevier SA, Amsterdam, **2004**.
[8] C. G. Young, in *Encyclopedia of Inorganic Chemistry 2*, vol. 5, Wiley, **2005**, p. 3321.
[9] *Metals in Biology*, vol. 39. *Molybdenum and Tungsten: Their Roles in Biological Systems* (Eds.: H. Segel, I. Segel), **2002**, Marcel Dekker, New York.
[10] K. D. Karlin, E. I. Stiefel (Eds.), *Progress in Inorganic Chemistry*, *Dithiolene Chemistry, Synthesis Properties and Applications*, vol. 52, Wiley, **2004**.
[11] J. H. Enemark, *Chem. Rev.* **2004**, *104*, 1175.
[12] J. L. Johnson, K. V. Rajagopalan, *Proc. Natl. Acad. Sci. USA* **1982**, *79*, 5414.
[13] S. P. Kramer, J. L. Johnson, A. A. Rebeiro, D. S. Millington, K. V. Rajagopalan, *J. Biol. Chem.* **1987**, *262*, 16357.
[14] M. K. Chan, S. Mukund, A. Kletzin, M. W. W. Adams, D. C. Rees, *Science* **1995**, *267*, 1463.
[15] B. Fischer, J. H. Enemark, P. Basu, *J. Inorg. Biochem.* **1998**, *72*, 13.
[16] J. L. Johnson, M. M. Wuebbens, K. V. Rajagopalan, *J. Biol. Chem.* **1987**, *264*, 13440.
[17] M. M. Wuebbens, K. V. Rajagopalan, *J. Biol. Chem.* **1993**, *268*, 13493.
[18] G. Schwarz, *Cell. Mol. Life Sci.* **2005**, *62*, 2792.
[19] M. M. Wuebbens, K. V. Rajagopalan, *J. Biol. Chem.* **1993**, *268*, 13493.

[20] M. M. Wuebbens, K. V. Rajagopalan, *J. Biol. Chem.* **1995**, *270*, 1082.
[21] P. Hänzelmann, H. Schindelin, *Proc. Natl. Acad. Sci. USA* **2004**, *101*, 12870.
[22] M. M. Wuebbens, M. T. W. Liu, K. V. Rajagopalan, H. Schindelin, *Structure* **2000**, *8*, 709.
[23] C. Rieder, W. Eisenreich, J. O'Brien, G. Richter, E. Götze, P. Boyle, S. Blanchard, A. Bacher, H. Simon, *Eur. J. Biochem.* **1998**, *255*, 24.
[24] J. A. Santamaria-Araujo, B. Fischer, T. Otte, M. Nimtz, R. R. Mendel, V. Wray, G. Schwarz, *J. Biol. Chem.* **2004**, *279*, 15994.
[25] M. J. Rudolph, M. M. Wuebbens, K. V. Rajagopalan, H. Schindelin, *Nat. Struct. Biol.* **2001**, *8*, 42.
[26] A. Matthies, K. V. Rajagopalan, R. R. Mendel, S. Leimkühler, *Proc. Natl. Acad. Sci. USA* **2004**, *101*, 5946.
[27] M. W. Lake, M. M. Wuebbens, K. V. Rajagopalan, H. Schindelin, *Nature* **2001**, *414*, 325.
[28] A. Matthies, M. Nimtz, S. Leimkühler, *Biochemistry* **2005**, *44*, 7912.
[29] G. Gutzke, B. Fischer, R. R. Mendel, G. Schwarz, *J. Biol. Chem.* **2001**, *276*, 36268.
[30] M. M. Wuebbens, K. V. Rajagopalan, *J. Biol. Chem.* **2003**, *278*, 14523.
[31] M. Aguilar, J. Cardenas, E. Fernandez, *Biochim. Biophys. Acta* **1992**, *1160*, 269.
[32] C. P. Witte, M. I. Igeno, R. Mendel, G. Schwarz, E. Fernandez, *FEBS Lett.* **1998**, *4321*, 205.
[33] F. S. Ataya, C. P. Witte, A. Galvan, M. I. Igeno, E. Fernandez, *J. Biol. Chem.* **2003**, *278*, 10885.
[34] J. A. Maupin-Furlow, J. K. Rosentel, J. H. Lee, U. Deppenmeier, R. P. Gunsalus, K. T. Shanmugan, *J. Bacteriol.* **1995**, *177*, 4851.
[35] S. Rech, C. Wolin, R. P. Gunsalus, *J. Biol. Chem.* **1996**, *271*, 2557.
[36] Y. Hu, S. Rech, R. P. Gunsalus, D. C. Rees, *Nat. Struct. Biol.* **1997**, *4*, 703.
[37] M. T. W. Liu, M. M. Wuebbens, K. V. Rajagopalan, H. Schindelin, *J. Biol. Chem.* **2000**, *275*, 1814.
[38] G. Schwarz, N. Schrader, R. R. Mendel, H.-J. Hecht, H. Schindelin, *J. Mol. Biol.* **2001**, *312*, 405.
[39] J. Kuper, A. Llamas, H.-J. Hecht, R. R. Mendel, G. Schwarz, *Nature* **2004**, *430*, 803.
[40] F. Blasco, J. Pommier, V. Augier, M. Chippaux, G. Giordano, *Mol. Microbiol.* **1992**, *6*, 221.
[41] S. Leimkühler, W. Klipp, *J. Bacteriol.* **1999**, *181*, 2745.
[42] M. J. Rudolph, M. M. Wuebbens, O. Turque, K. V. Rajagopalan, *J. Biol. Chem.* **2003**, *278*, 14514.
[43] M. W. Lake, C. A. Temple, K. V. Rajagopalan, H. Schindelin, *J. Biol. Chem.* **2000**, *275*, 40211.
[44] T. Palmer, C.-L. Santini, C. Lobbi-Nivol, D. J. Eaves, D. H. Boxer, *Mol. Microbiol.* **1996**, *20*, 875.
[45] V. Massey, D. E. Edmondson, *J. Biol. Chem.* **1970**, *245*, 6595.
[46] T. Nishino, C. Usami, K. Tsushima, *Proc. Natl. Acad. Sci. USA* **1983**, *80*, 1826.
[47] L. Xiong, M. Ishitani, H. Lee, J.-K. Zhu, *Plant Cell* **2001**, *13*, 2063.
[48] F. Bittner, M. Oreb, R. R. Mendel, *J. Biol. Chem.* **2001**, *276*, 40381.
[49] L. Zheng, R. H. White, V. L. Cash, R. F. Jack, D. R. Dean, *Proc. Natl. Acad. Sci. USA* **1993**, *90*, 2754.
[50] T. Heidenreich, S. Wollers, R. R. Mendel, F. Bittner, *J. Biol. Chem.* **2005**, *280*, 4213.
[51] J. J. Truglio, K. Theis, S. Leimkühler, R. Rappa, K. V. Rajagopalan, C. Kisker, *Structure* **2002**, *10*, 115.
[52] H. Dobbek, L. Gremer, O. Meyer, R. Huber, *Proc. Natl. Acad. Sci. USA* **1999**, *96*, 8884.
[53] I. Bonin, B. M. Martins, V. Pruvanov, S. Fetzner, R. Huber, H. Dobbek, *Structure* **2004**, *12*, 1425.
[54] M. J. Romão, M. Archer, I. Moura, J. J. G. Moura, J. LeGall, R. Engh, M. Schneider, P. Hof, R. Huber, *Science* **1995**, *270*, 1170.
[55] R. Huber, P. Hof, R. O. Duarto, J. J. G. Moura, I. Moura, M.-Y. Liu, J. LeGall, R. Hille, M. Archer, M. J. Romão, *Proc. Natl. Acad. Sci. USA* **1996**, *93*, 8846.
[56] R. M. Jones, F. E. Inscore, R. Hille, M. L. Kirk, *Inorg. Chem.* **1999**, *38*, 4963.
[57] S. W. Ragsdale, *Crit. Rev. Biochem. Mol. Biol.* **2004**, *39*, 165.
[58] R. K. Watt, P. W. Ludden, *Cell. Mol. Life Sci.* **1999**, *56*, 604.
[59] H. Dobbek, L. Gremer, R. Kiefersauer, R. Huber, O. Meyer, *Proc. Natl. Acad. Sci. USA* **2002**, *99*, 15971.
[60] M. Gnida, R. Ferner, L. Gremer, O. Meyer, W. Meyer-Klaucke, *J. Biochem.* **2003**, *42*, 222.
[61] K. Okamoto, K. Matsumoto, R. Hille, B. T. Eger, E. F. Pai, T. Nishino, *Proc. Natl. Acad. Sci. USA* **2004**, *101*, 7931.
[62] T. D. Tullius, D. M. Kurtz, S. D. Conradson, K. O. Hodgson, *J. Am. Chem. Soc.* **1979**, *101*, 2776.
[63] J. Bordas, R. C. Bray, C. D. Garner, S. Gutteridge, S. Hasnain, *Biochem. J.* **1983**, *191*, 499.
[64] R. Hille, H. Sprecher, *J. Biol. Chem.* **1987**, *262*, 10914.
[65] K. N. Murray, J. G. Watson, S. Chaykin, *J. Biol. Chem.* **1966**, *241*, 4798.
[66] M. Xia, R. Dempski, R. Hille, *J. Biol. Chem.* **1999**, *274*, 3323.
[67] R. J. Greenwood, G. L. Wilson, J. R. Pilbrow, A. G. Wedd, *J. Am. Chem. Soc.* **1993**, *115*, 5385.
[68] B. D. Howes, R. C. Bray, R. L. Richards, N. A. Turner, B. Bennett, D. J. Lowe, *Biochemistry* **1996**, *35*, 1432.
[69] C. J. Doonan, A. L. Stockert, R. Hille, G. N. George, *J. Am. Chem. Soc.* **2005**, *127*, 4518.
[70] E. I. Stiefel, *Proc. Natl. Acad. Sci.* **1977**, *70*, 988.
[71] E. I. Stiefel, *Prog. Inorg. Chem.* **1977**, *22*, 1.
[72] R. B. McWhirter, R. Hille, *J. Biol. Chem.* **1991**, *266*, 23724.
[73] R. C. Bray, G. Palmer, H. Beinert, *J. Biol. Chem.* **1964**, *239*, 2667.
[74] R. C. Bray, T. Vånngärd, *Biochem. J.* **1969**, *114*, 725.
[75] S. J. Tanner, R. C. Bray, F. Bergmann, *BioChem. Soc. Trans.* **1978**, *6*, 1328.
[76] D. Edmondson, D. Ballou, A. van Heuvelen, G. Palmer, V. Massey, *J. Biol. Chem.* **1973**, *248*, 6135.
[77] R. C. Bray, G. N. George, *BioChem. Soc. Trans.* **1985**, *13*, 560.
[78] J. P. G. Malthouse, G. N. George, D. J. Lowe, R. C. Bray, *Biochem. J.* **1981**, *199*, 629.
[79] S. Gutteridge, R. C. Bray, *Biochem. J.* **1980**, *189*, 615.
[80] P. Manikandan, E.-Y. Choi, R. Hille, B. M. Hoffman, *J. Am. Chem. Soc.* **2001**, *123*, 2658.
[81] G. A. Lorigan, R. D. Britt, J. H. Kim, R. Hille, *Biochim. Biophys. Acta* **1994**, *1185*, 284.
[82] M. D. Davis, J. S. Olson, G. Palmer, *J. Biol. Chem.* **1982**, *257*, 14730.
[83] M. D. Davis, J. S. Olson, G. Palmer, *J. Biol. Chem.* **1984**, *259*, 3526.
[84] R. Hille, G. N. George, M. K. Eidsness, S. P. Cramer, *Inorg. Chem.* **1989**, *28*, 4018.
[85] J. H. Kim, M. G. Ryan, H. Knaut, R. Hille, *J. Biol. Chem.* **1996**, *271*, 6771.
[86] R. C. Bray, P. F. Knowles, *Proc. R. Soc. London, Ser. A* **1968**, *302*, 351.
[87] C.-H. Lee, E. B. Skibo, *Biochemistry* **1987**, *26*, 7355.
[88] A. A. Voityuk, K. Albert, S. Kostlmeier, V. A. Nasluzov, K. M. Neyman, P. Hof, R. Huber, M. J. Romão, N. Rösch, *J. Am. Chem. Soc.* **1997**, *119*, 3159.
[89] A. A. Voityuk, K. Albert, M. J. Romão, R. Huber, N. Rösch, *Inorg. Chem.* **1998**, *37*, 176.
[90] P. Ilich, R. Hille, *J. Phys. Chem. B* **1999**, *103*, 5406.
[91] P. Ilich, R. Hille, *J. Am. Chem. Soc.* **2002**, *124*, 6796.
[92] C. C. Page, C. C. Moser, X. Chen, P. L. Dutton, *Nature* **1999**, *402*, 47.
[93] A. L. Stockert, S. Shinde, R. F. Anderson, R. Hille, *J. Am. Chem. Soc.* **2002**, *124*, 14555.

[94] S. Leimkühler, R. Hodson, G. N. George, K. V. Rajagopalan, *J. Biol. Chem.* **2003**, *278*, 20802.
[95] T. Nishino, Y. Amaya, S. Kawamoto, Y. Kashima, K. Okamoto, T. Nishino, *J. Biol. Chem.* **2002**, *132*, 597.
[96] S. Leimkühler, A. L. Stockert, K. Igarashi, T. Nishino, R. Hille, *J. Biol. Chem.* **2004**, *279*, 40437.
[97] N. C. Maiti, T. Tomita, T. Kitagawa, K. Okamoto, T. Nishino, *J. Biol. Inorg. Chem.* **2003**, *8*, 327.
[98] C. Hemann, P. Ilich, A. L. Stockert, E.-Y. Choi, R. Hille, *J. Phys. Chem. B* **2005**, *109*, 3023.
[99] C. Enroth, B. T. Eger, K. Okamoto, T. Nishino, T. Nishino, E. F. Pai, *Proc. Natl. Acad. Sci. USA* **2000**, *97*, 10723.

Received: January 27, 2006
Published Online: April 25, 2006

